TÜBİTAK

Turkish Journal of Chemistry

http://journals.tubitak.gov.tr/chem/

Review Article

Turk J Chem
(2018) 42: 587 – 610
© TÜBİTAK
doi:10.3906/kim-1611-35

Recent advances in organ-on-a-chip technologies and future challenges: a review

Hüseyin AVCI[1,*], Fatma DOĞAN GÜZEL[2], Salim EROL[3], Ali AKPEK[4]

[1]Department of Metallurgical and Materials Engineering, Eskişehir Osmangazi University, Eskişehir, Turkey
[2]Department of Biomedical Engineering, Ankara Yıldırım Beyazıt University, Ankara, Turkey
[3]Department of Chemical Engineering, Eskişehir Osmangazi University, Eskişehir, Turkey
[4]Harvard-MIT Division of Health Sciences & Technology, Boston, MA, USA

Received: 15.11.2016 • **Accepted/Published Online:** 17.05.2017 • **Final Version:** 01.06.2018

Abstract: The significant development in the construction of microscale cell culture platforms and the interest in bioanalytical analysis have recently resulted in the emergence of a new concept of 'organ-on-a-chip' systems. Organ-on-a-chip is a new three-dimensional (3D) in vitro microfabricated unit that contains a multichannel microfluidic cell culture. Even if many informative and useful data are obtained from animal models and in vitro assays, they are still limited for extrapolation to human systems during drug design and development. Only about 1 out of 10,000 compounds is processed in clinical trials for final approval. As being the first example of its kind, in this review, we summarize the current status and future challenges of this new concept that is a promising radical improvement in the drug-monitoring field. In addition, 3D-bioprinting methods used for the construction of organs-on-chips are outlined within the context in order to address the complexities in the field and show the various ways to create these semiartificial hybrid devices using a multidisciplinary approach comprising chemistry, biology, and engineering.

Key words: Organ-on-a-chip, 3D bioprinting, drug screening, in vitro cell culture

1. Introduction

It is well known that the determination of the absorption, distribution, metabolism, and elimination of a drug in the human body is a very complex process and needs highly sophisticated methods and tools.[1–7] During these processes, the investigation of a correlation between concentration and time of the initial-loaded drug in the bloodstream and in the tissues of organs is very crucial to understand the interaction and the effects of the drug in the body. An important approach toward these interaction profiles is using and analyzing some mathematical models. For example, Shuler[8] developed a pharmacokinetic–pharmacodynamic (PK-PD) model to correlate data obtained from organs-on-chips with the data from in vivo experiments. In addition, Sung et al. combined PK-PD modeling with a microscale cell culture analog, which is an in vitro experimental approach, to comprehend the mechanism of drug toxicity.[6] Bhise et al. suggested that computational fluid dynamics models can provide a mechanistic understanding of drug delivery in organ-on-a-chip systems.[9]

Cost and time are two important parameters for investigating and developing new drugs. It takes about 12 to 15 years to develop a new drug, and only a few of these drugs are approved by the authorities.[7] Various reasons for failure in drug development attempts are directly related to the lack of efficacy and their severe side effects, which could not be observed by current in vivo and in vitro models.[5,7] In vitro cell or tissue culture

*Correspondence: havci@ogu.edu.tr

models can give the first indication of the efficacy and toxicity of the drug for physiological and pathological responses.[5] If in vitro results are promising, the effect of the compound can be investigated by using animal models. However, these two models have crucial shortcomings. For example, in vitro models do not represent complex cell–cell and cell–matrix interactions, which may result in inaccurate diagnostic bias.[5] Some candidate compounds can be effective in vitro but ineffective in vivo because of the complex interactions between the drug and the biological environment, especially in cells and tissues. The unforeseen lack of efficacy or toxicity, which is not revealed in vitro studies, is one of the important reasons for the high attrition rate. Therefore, a very high rate of failure and expenses associated with the drug development research occur in the later clinical investigations of phases II and III.[6,7]

Therefore, it is important to conduct appropriate and precise experiments before the clinical trials that can also help to reduce cost and time tremendously. In order to solve this problem, the 'organ-on-a-chip' concept has been developed as an alternative in vitro technique. Organs-on-chips closely mimic human tissues and organs by using multichannel 3D microfluidic and other microfabricated structures that give the opportunity to observe the activities, mechanics, and physiological responses as observed for human organs.[4,5,10] It is believed that experimentation with animal testing could soon be replaced by some of these sophisticated organ-on-a-chip models. It is also foreseen that this would pave the way forward for the development of inexpensive and fast testing of potentially new diagnostic and therapeutic approaches. In this technology, the microstructures behave as scaffolding for the growth of human cells and provide an interaction between the cells and the molecules such as drug particles and ions.

Recent technological advancements have been invaluable to understand the functioning of artificial organs (i.e. heart, kidneys, liver, lung, and vessels). This in vitro progress has enabled cellular environments closely mimicking the properties of human tissues and organs in many aspects. The next achievement was the integration of these artificial microengineered tissues and organs with stem cell technology to obtain 'body- or human-on-a-chip' systems and to observe the effects of drugs on the human body during the proposed treatment period. The use of such systems will considerably reduce the time and cost of the development of novel drugs and associated treatment in the pharmaceutical and medical industries.[5,11,12]

In this review, briefly, recent advances in in vitro tissue culture models, organ-on-a-chip platforms, and their physiological relevance are presented. The review also provides exclusive information about the current and future challenges. The final section is dedicated to the various 3D bioprinting technologies used in the field so that a complete understanding of the subject is reached.

2. Recent developments in organ-on-chip technologies

In this section, specific examples of the latest research efforts for mimicking the kidneys, lungs, heart, blood vessels, and liver are outlined to demonstrate the use of these platforms. Furthermore, as a new and promising technology for tissue model development, recent 3D bioprinting technologies are highlighted in the next section. Material, mathematical, and physical simulation necessities in order to advance organ-on-a-chip technologies and finally the significant advantages are mentioned in Section 4.

2.1. Kidney-on-a-chip

The kidney is one of the most complicated organs in the human body; therefore, it is an enormous challenge for researchers to develop a platform of 'kidney-on-a-chip' that can mimic its function partially or fully when exposed to various drugs and medications.

The nephron is the functional and basic structural unit of the kidney. It regulates the concentration of water and soluble substances during filtering of our blood, and the desired substances for our body are reabsorbed while excreting the remaining ones as urine.[11] A nephron can be divided into three main sections, in which the blood first enters the glomerulus, where the passive mechanical filtration occurs to hold the cells and large proteins. In the second section, the blood and filtrate flow reach the proximal tubule where the reabsorption process takes place. The filtration process is completed in the loop of Henle by osmosis, diffusion, and reabsorption. The filtrate is eventually transferred to the collecting duct system after passing through the distal convoluted tubule, responsible for the regulations of ions and pH, and is processed there to form concentrated waste urine.[13]

An on-chip nephron device made out of a single multilayered polymer construct has been proposed by Weinberg et al.[14] The chip resembles the functioning nephron with these three sections, namely the glomerulus, the proximal tubule, and the loop of Henle, as shown in Figure 1. It is made up of two microfabricated layers separated by a membrane. The filtration of the glomerular unit, the reabsorption in the tubule, and the large increase in urea concentration in the loop of Henle were all observed when a blood sample was introduced into the on-chip nephron device. This was one of the first attempts in the field. Though it was a successful attempt, there were challenges to be addressed related to the culture and control of the various cell types, and the filtration process for the separation of waste was not as efficient as for the normal nephron.

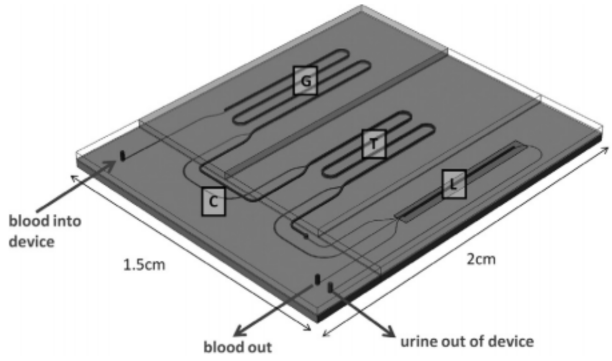


Figure 1. Schematic representation of the nephron device (reprinted with permission from Weinberg et al.; copyright (2008), Wichtig Publishing[14]).

Jang et al. developed a polydimethyl siloxane (PDMS)-based microfluidic device with a porous membrane substrate sandwiched in the middle.[13] It was designed to proliferate and investigate renal cells of the tubule of the kidney, as shown in Figure 2. In this model, primary rat inner medullary collecting duct (IMCD) cells were cultured in the microfluidic channels, and the optimum environmental conditions for the cells were obtained by the application of an appropriate fluidic shear stress for a certain time. Under these conditions of fluidic shear stress, the cultured IMCD cells exhibited improved alignment of the cytoskeleton, cell polarization, cell junctions, and hormonal stimulations initiated regulating water and ion balance by molecular transport when compared with the same cell type cultured statically.

Another research group recently reported an alternative version of the chip in order to construct 'in vivo-like' proximal tubular morphology for the study of renal toxicity.[15] Their work is the first of its kind that uses primary human kidney proximal tubular epithelial cells in a microfluidic device exploring nephrotoxicity under dynamic fluidic flow. A PDMS-based microfluidic device is separated by a porous (pore size: 0.4 mm) polyester membrane, as seen in Figure 3. This structure closely resembles the flow mechanism of the tubular

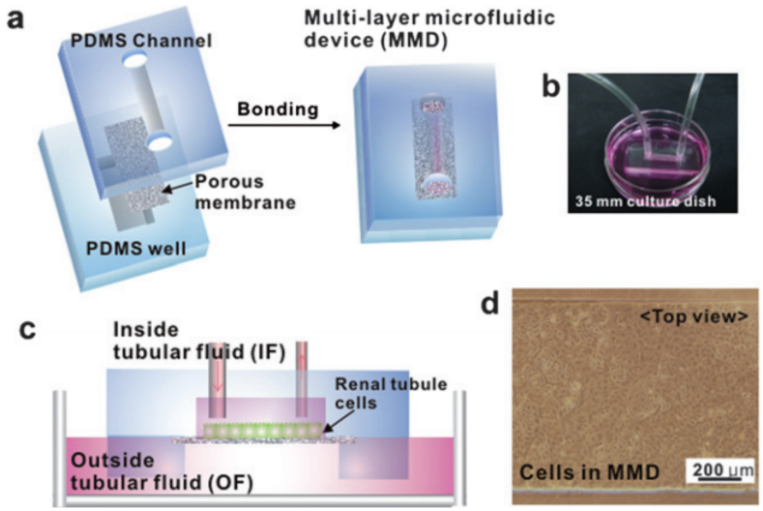


Figure 2. Schematic of the MMD device: (a) assembly of the device by plasma treatment; (b) working principle of the MMD device on a culture dish that has a syringe pump with silicone tubes; (c) schematic of the functional device; (d) a microscope image of primary cultured rat IMCD cells within the inside channel of MMD after seeding for 3 days (reprinted with permission from Jang et al.; copyright (2010), The Royal Society of Chemistry [13]).

flow of interstitial fluid at the tissue–tissue interface of the kidney proximal tubule. The upper surface of the extracellular matrix (ECM)-coated membrane was seeded and spread by the epithelial cells, and then the compartment was filled with the culture medium, flowing with a low level of shear stress. The lower section of the device was loaded with the culture medium in order to form a similar environment for the interstitial space of the kidney.

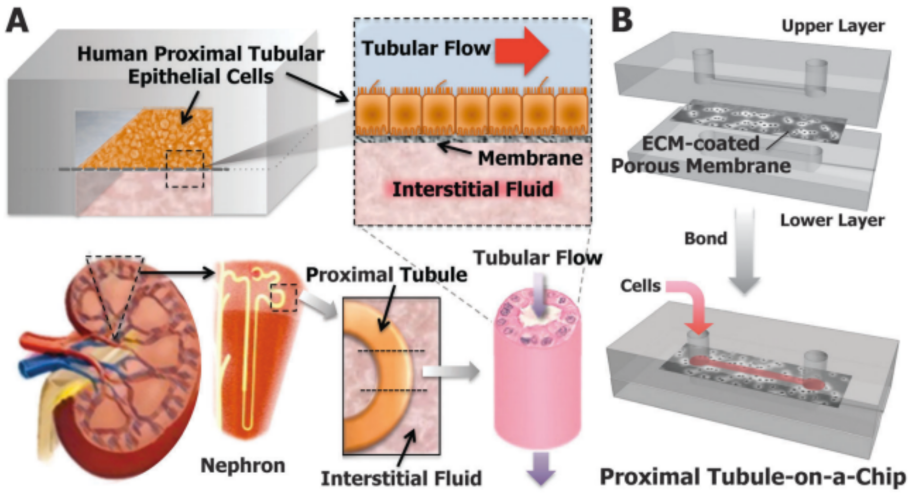


Figure 3. Microdevice engineering of human kidney proximal tubule-on-a-chip: (A) schematic representation of intraluminal channel and interstitial space, which is divided by an ECM-coated porous membrane. Human proximal tubule epithelial cells are plated on the porous membrane active and passive epithelial transport similar to the living kidney proximal tubule. (B) Schematic of the device assembly; top microfluidic channel, ECM-coated porous membrane, and lower microfluidic channel combined together by the treatment of surface plasma. Cells are placed through device inlet. Inlets show the structure of the tubular flow in nephron (reprinted with permission from Jang et al.; copyright (2013), The Royal Society of Chemistry [15]).

The number of cells expressing primary cilia was also tremendously increased when they were exposed by the apical shear stress. It is known that the primary cilia are one of the essential parts for fluid mechanosensing and regulation of tubular morphology. Another interesting use of the device was the ability to determine the physiological transport functions by observing the albumin uptake rate from the apical medium under static and fluidic conditions. Under appropriate fluidic conditions, the albumin uptake percent could be improved by more than double, making the device an in vivo-like phenotype. Toxicity tests were also carried out by injecting cisplatin, which is a chemotherapeutic drug, into the interstitial part of the microdevice to observe the effects of conditions in terms of cell injury as determined by lactate dehydrogenase release. The presence of flow significantly improved the response of the toxicity of the cells; they were healthier when compared with the cells cultured under static conditions. As a result, this microdevice model can give more accurate information for those working on kidney diseases and nephrotoxicity, as well. Furthermore, it is important to mention that this model is one of the first to use primary human kidney proximal tubular epithelial cells to compare the transport activities between static and fluidic culture environments.

A 3D bioprinting of convoluted proximal tubules was shown in a recent work.[16] Here, the proximal tubule construct was fabricated using a 3D bioprinter. This method provides enhanced epithelial morphology and functional properties compared to 2D constructs. Additionally, the same methodology can be applied to produce other parts of the nephron, such as the distal convoluted tubule or loop of Henle.

2.2. Lung-on-a-chip

The lung is the primary organ in the respiratory system. In the normal human respiratory system, the trachea transfers the inhaled air into the lungs through the tubular branches, also called bronchi. Bronchi are divided into smaller branches ending with the alveoli, where the exchange of gases occurs. Oxygen passes from the air into the blood, and similarly carbon dioxide passes from the bloodstream into the atmosphere through the alveoli. Alveoli are covered with capillaries carrying the blood plasma. The membrane at the interface between alveoli and capillaries consists of epithelial cells from the alveoli side and endothelial cells from the capillary side.[11] The human airway epitheliums (e.g., ciliated, mucous, type I and type II cells in the alveolar epithelium) have unique physicochemical and immune barriers between the host and the environment and are able to respond to a wide range of outcomes.[17–19] For example, the interaction of a receptor (Fas (CD95)) and its ligand (FasL) in the airway epithelium can act as an immune barrier in which the apoptosis of cells is initiated.

Studying lungs-on-microchips can offer a new pathway in order to analyze airborne diseases and to screen therapeutic effects of the associated drugs. It is important because of the considerable increase in air pollution, especially in developing countries, and the eventual increase in lung-associated illnesses. One of the first 'lungs-on-chips' was designed with inspiration from human breathing.[20] It was formed by two closely apposed microchannels separated by a flexible, porous, and very thin (10 μm) membrane manufactured from PDMS. The membrane in between was coated with ECM (consisting of fibronectin or collagen). The schematic of the device is shown in Figure 4. Human alveolar epithelial cells and human pulmonary microvascular endothelial cells were cultured on the opposite sides of the membrane. The air was introduced into the epithelial compartment, while the bottom microchannel filled with endothelial cells was infused with a blood-like liquid. A vacuum was applied to the microchambers to enable mechanical stretching of the PDMS membrane mimicking human breathing. The proposed system delivers the fluid flow well, distributing cells and nutrients to the epithelium and endothelium. In addition to the study of alveolar epithelial and endothelial cells, they used immune cells in

order to obtain similar human lung responses to infection and inflammation triggered by inhaled pathogens. It is clear that the chip demonstrates a low-cost screening model that could potentially replace currently available in vivo assays.

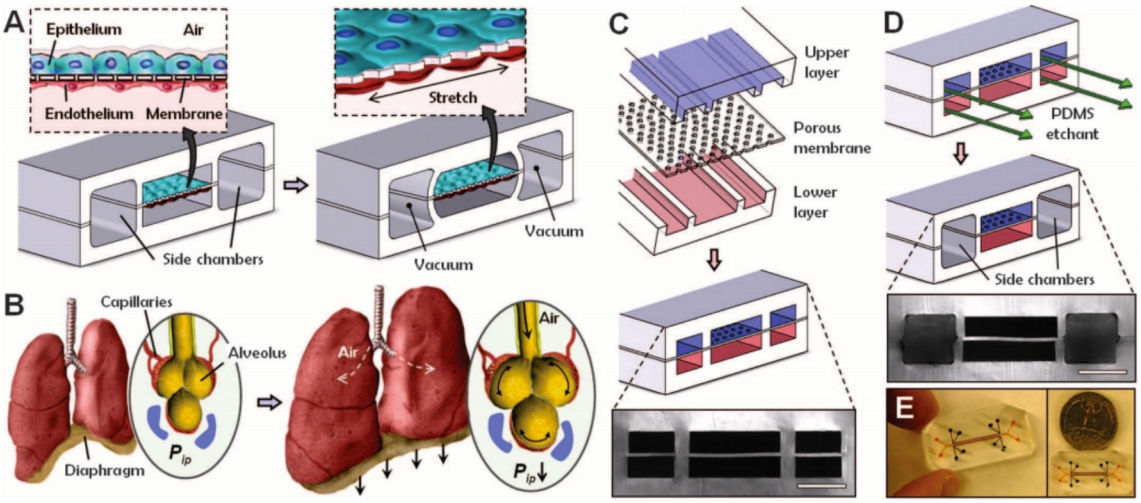


Figure 4. Schematic representation of a lung-on-a-chip microdevice: (A) schematic of the device: device consists of PDMS microchannels with ECM-coated porous and flexible PDMS membrane representing an alveolar-capillary barrier. Vacuum is applied to the side chambers to obtain mechanical stretching to mimic the alveolar-capillary barrier. (B) Schematic of the lung working principles: upon inhalation intrapleural pressure decreases while the alveolar-capillary interface stretches due to the tension of the alveoli. (C) Device construction: upper and bottom microchannels with a membrane in between are bonded together with plasma exposure. (D) PDMS etchant is used in the side chambers to remove the membrane for vacuum applications. (E) Photography images of lung-on-a-chip microdevice. Scale bar: 200 μm (reprinted with permission from Huh et al.; copyright (2010), American Association for the Advancement of Science[20]).

Another group of researchers produced a lung-on-a-chip microdevice to improve the physiological relevance of existing in vitro alveolar capillary interface models.[21] They successfully cultured alveolar epithelial cells at an air–liquid interface with continuous nutrient perfusion and this also showed a higher degree of monolayer integrity and a decrease in surface tension of the hypophase. The production steps of a multilayer microfluidic cell-culture device are shown Figure 5 in detail. In general, porous polyethylene terephthalate (PET) membrane (pore size: 0.4 mm) was sandwiched between the bottom and the top layer of PDMS in the microdevice. Afterwards, a mixed liquid of PDMS as a curing agent for the prepolymer was used to bond the layers together, followed by a final curing step under a suitable heating process. The human alveolar epithelial cells were placed on the top and bottom of the PET culture wells of the device.

To determine the cell monolayer integrity under different culture conditions (i.e. atmospheric air, culture media) transepithelial electrical resistance (TEER) measurements were carried out, and it was found that the cells indicated tight junctions under both conditions. However, the air-exposed cultures demonstrated higher TEER values than the cells cultured in media. In addition to TEER observations, sodium fluorescein uptake for permeability studies was investigated under the two abovementioned culture conditions. Reduction in permeability was higher for air-exposed cells than that for the cultured cells. This indicated better cell viability and monolayer integrity for the air-exposed cultures.

Use of such a device brings the advantages of good integrity of closely packed cells, efficient waste removal

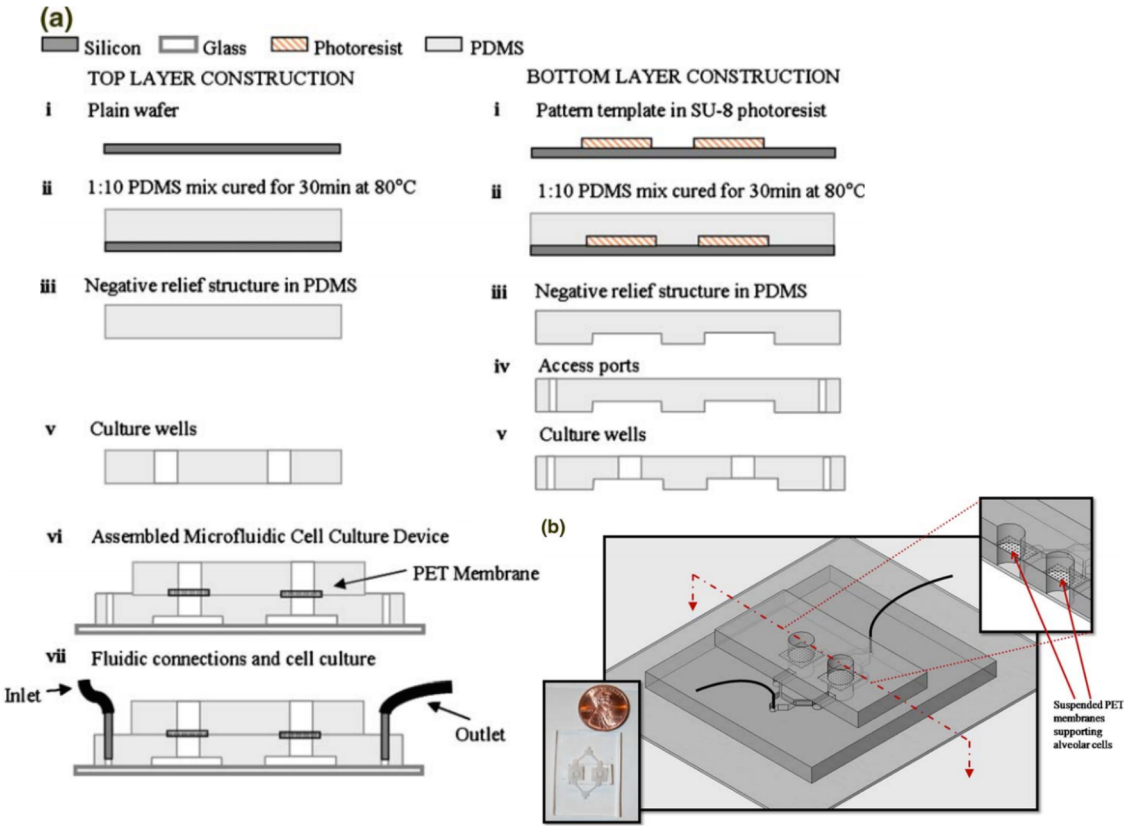


Figure 5. (a) Illustration of production steps for the microfluidic device: (i) preparing for the formation of a light-sensitive film used for photolithography (SU-8) on silicon wafer; (ii) the curing process of liquid PDMS with 1:10 ratio of curing agent to prepolymer mix on the SU-8 substrate for 30 min at 80 °C; (iii) negative relief structure in PDMS slab to obtain small holes; (iv) placing the access ports in the PDMS mold; (v) formation of the culture wells; (vi) assembling the device by bonding the bottom PDMS layer to a glass slide via exposure of O_2 plasma for 2 min at 25 W and then heating at 80 °C for 1 h; (vii) final device structure with fluidic connections to the lower PDMS layer and cell culture. (b) Images of an actual and a schematic display of the multilayer microfluidic cell-culture device with the cross-sectional view of red dotted line that shows suspended PET membranes supporting alveolar cells (reprinted with permission from Nalayanda et al.; copyright (2009), Springer International Publishing[21]).

and constant nutrient replenishment, and a lower surface tension of the hypophase with the consistently higher presence of surfactant during cell growth. In addition, the device is an open-access model where one can study different cell culture models, drugs, and treatment systems experiencing dynamic forces. All of the above make this model a promising tool imitating the physiological environment of the lung similarly to the real one.

2.3. Heart-on-a-chip

The cardiovascular system has a crucial function in the human body, consisting of the heart, blood, blood vessels, and lymphatic system. They are mainly responsible for the transport of O_2, CO_2, nutrients, cellular waste, and hormones throughout the body. The heart is a vital part of the cardiovascular system and is the body's hardest working organ due to working for the entire life without stopping to pump the blood throughout the entire body. It is located more to the left of the breastbone in the middle mediastinum and connects to the largest artery, the aorta, in the human body. The heart manages many sensitive processes in the body very

well; for example, it controls the synchronized contraction of the individual myocytes (also known as muscle cells) in a certain period of time and the opening of the valves without any leak. During diastole, the ventricles are filled with blood properly, and the degree of contractions is sufficiently adequate.[22] The heart includes permanent cells, such as cardiomyocytes, cardiac fibroblasts, and endothelial cells, and transient cell groups, which include lymphocytes, mast cells, and macrophages.[11] These two groups of permanent and transient cells have interactions between each other and these interactions influence the function of the cardiac system.

In the past, in general, the correlation between electrophysiological and contractility properties of cardiac cells was observed from a single cardiomyocyte. It is clear that the cultures of cardiac myocytes do not give the whole response and the structure of the cardiac tissue, and some functions should be protected, such as contractility and the ion channel composition of the original cells.[23] In addition, to obtain more accurate data, there should be at least a single or multiple tissue scale systems. Grosberg et al. reported obtaining a 'heart-on-a-chip' based on a muscular thin film (MTF) technique that comprised a ventricular myocardium on an elastomeric thin film.[24] The contractility for up to eight MTFs and cytoskeletal construction for multiple tissues were achievable. Therefore, it is a significant example providing the relation between structure and function and simulating the architecture of laminar cardiac muscle. In this study, after the production of the MTF chips, the surface was spin-coated with poly(N-isopropylacrylamide) (PIPAAm) and later coated by PDMS, as shown in Figure 6. An ECM protein, fibronectin, was utilized to provide guidance cues for self-assembly of myocytes. The myocytes were then seeded on the substrates and cultured for a certain time prior to conducting the experiments.

An external field stimulator with a digital video was used in order to analyze each contraction cycle and monitor the systolic and diastolic stresses. In addition, different concentrations of a dose of epinephrine, electrophysiological mapping, and immunofluorescent staining (e.g., actin, nuclei) were studied to analyze pharmacological responses. As a result, one can say that this chip technology with various cell-culturing models has shown an investigation of stress and electrophysiological activity. It also well resembles the cellular architecture in healthy, diseased, and developing cardiac tissues.

Another novel engineered heart prototype was reported by Agarwal et al.[25] Their work showed a laser-induced fabrication of thin PDMS cantilevers. Some advantages of this MTF technology over conventional ones can be summarized as mimicking the similar response of in vivo physiology, contractility, and electrophysiological properties. The use of autoclavable materials was also a plus here, which prevented the absorption of drug molecules during the in vitro drug treatment. It should be noted that the team obtained similar data of average peak systolic and twitch stress for each MTF after each contraction until four cycles (Figure 7) in MTF experiments, which were isolated rat papillary muscle contractility experiments performed in an open-well configuration. Furthermore, the higher reproducibility rate of the MTF technology, the opportunity to work with different types of cell sources (i.e. primary human cardiomyocytes), and the simultaneous observation of multiple tissue responses for the study of contractility properties under different exposure regimes during the treatment with and without drugs were some other advantages of the device. This was also one of the first designs that would potentially enable the mimicking of diseased organs by the perfusion of suitable target molecules.

Mechanical and biological properties of cardiac muscle cells such as alignment, elongation, and growth properties should be considered when designing artificial cardiac tissue. In this regard, there are also some important studies showing the production and analysis of hydrogel-based microarchitecture designs for probing the structure and functional properties of actual cardiac tissue under physiological conditions.[26–29] Hydrogels

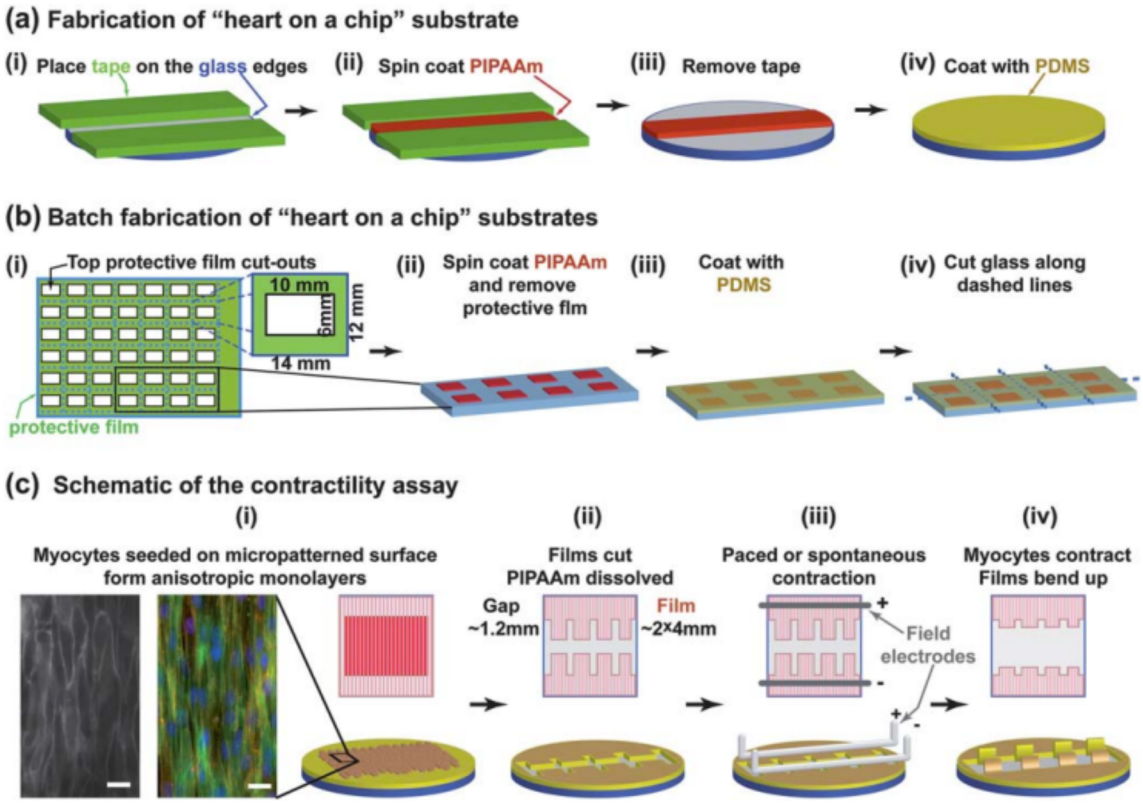


Figure 6. Schematic of systematic fabrication of heart-on-a-chip: (a) production of single 25-mm-wide round template; (b) batch production of the templates; (c) contractility assay development: neonatal rat ventricular myocytes are seeded on the surface of the functionalized substrate. Bottom row shows the 3D schematic representation, top row is the top view of the design, and left is voltage-sensitive dye for membrane dye staining (staining agent used in immunostaining for α-actinin – red, actin – green, nuclei – blue (right image)). Scale bar is 20 μm (reprinted with permission from Grosberg et al.; copyright (2011), The Royal Society of Chemistry [24]).

demonstrate a microstructure very similar to the native ECMs with tunable mechanical properties like allowing transport of nutrients, wastes, and high oxygen content. Among the controllable features, the properties of hydrogels are those to provide biological communication for cells, biodegradability, and ease for the transport of solutes. Consequently, synthesis of hydrogels with various chemical and physical properties for regenerative medicine, tissue engineering, and biomimetic tissue construction applications has been increasing rapidly. [28] Furthermore, many published studies related to direct and indirect patterning to precisely control the spatial position of the cells within the hydrogel only barely achieved the spatial location and proper control over the cell density. More recently, Naseer et al. demonstrated an acoustic-based technique called surface acoustic waves (SAWs) to pattern the cardiac cells in a quick, controllable, and contactless fashion within gelatin methacryloyl (GelMA). [29] The standing SAW-induced energy transferred into the gel was used to position and align the cells less than 10 s before photo-crosslinking the chains of GelMA. They successfully observed beating activity less than a week after the cell alignment and spreading.

Annabi et al. developed functional cardiac tissue models via photo-crosslinking of methacrylated tropoelastin (MeTro) in order to mimic its dynamic properties. [30] They also studied the behavior of cardiomyocyte attachment, alignment, spreading, and communication. For these novel engineered micropatterned elastic gels,

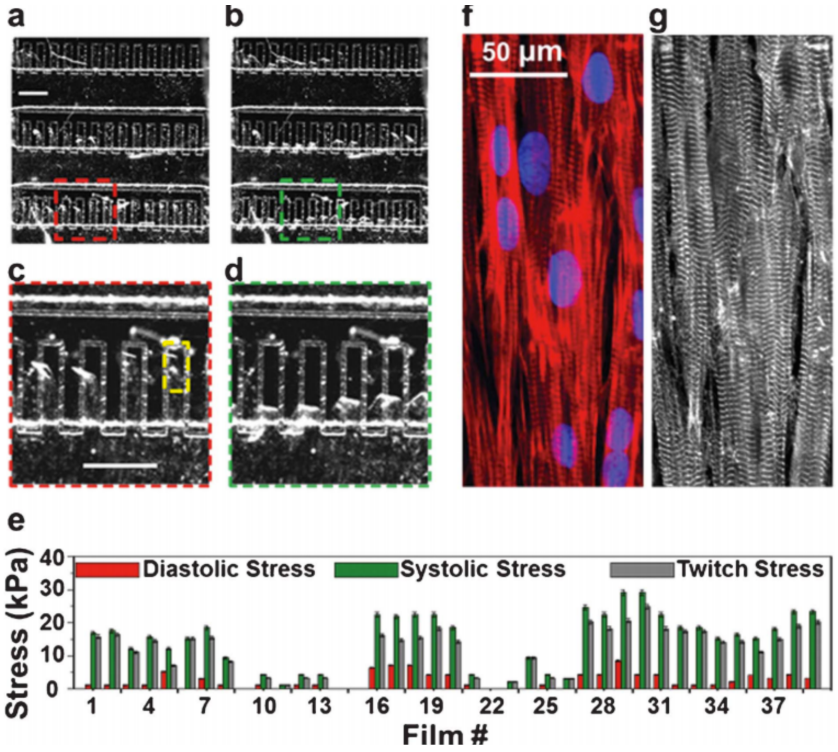


Figure 7. Images and graph for the proposed heart-on-a-chip design: (a) bright-field image for the performance of the chip during diastole and (b) peak systole with scale bar of 1 mm; (c) and (d) show the higher magnification of (a) and (b) with scale bar of 1 mm; (e) graph showing diastolic, peak systolic, and twitch stress response for each MTF design (e.g., an average twitch stress after 35 replicates is 12.7 $\pm$ 1.1 kPa by using one higher-throughput chip); (f) fluorescent image for immunostaining of the actin filaments and nuclei (represent by red and blue, respectively); (g) represents the region highlighted as a yellow rectangle in (c) and demonstrates sarcomeric α-actinin for the generation of an anisotropic monolayer for the cardiac tissue (reprinted with permission from Agarwal et al.; copyright (2013), The Royal Society of Chemistry [25]).

a human protein of water-soluble tropoelastin, which consists of 35 lysine residues per molecule, was used in the formation of highly elastic MeTro gel. This gel also has high-resolution microchannels on the surface, as seen in Figure 8. Higher elongation at break up to 400% and tensile modulus of about 15 kPa, which is close to the modulus of rat CMs of 30 kPa, were some important results produced using MeTro hydrogel. In fact, UV exposure times, the components' concentrations in MeTro gel, channel width, and culture time should be carefully controlled and optimized to obtain well-defined microscale structures mimicking the native rat heart. After CM attachment on MeTro hydrogel, a higher rate of cell proliferation, an anisotropic arrangement with sufficient spreading ability, and a confluent cell layer elongation were observed. In terms of the immunohistochemical detection capability of the gel, it can be seen that a well-defined sarcomere structure forms a formation similar to the ventricular myocardium of a native adult rat. Additionally, there was not any significant change in the beat frequency across the culture time; a consistently synchronized beating of systole and diastole could be maintained at least 2 weeks in response to optimized electrical field stimulation. It would be conceivable to think that further development of the system, which also includes intercalated disk and gap junctions between myocytes with higher alignment and elongation of cardiac troponin I (cTnI), would potentially lead to it resembling the native myocardium more.

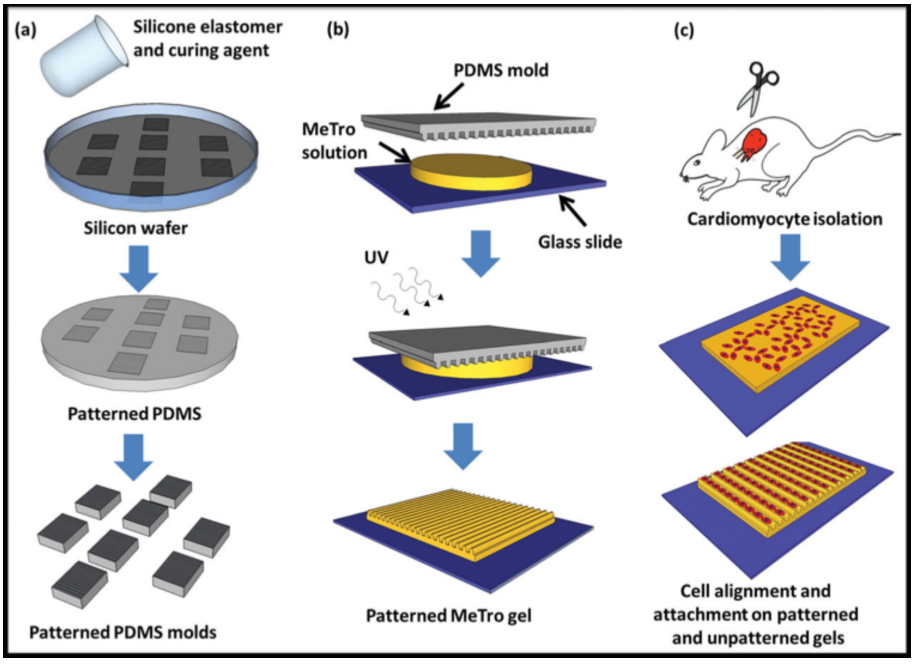


Figure 8. Illustrations of production process for patterned PDMS molds, MeTro gel, and cardiomyocyte alignment and attachment on the gels: (a) producing patterned PDMS molds; (b) manufacturing micropatterned MeTro gel by placing the molds in MeTro and photoinitiator solution placed on a glass slide, UV light exposure for crosslinking, and then the PDMS removal; (c) cell alignment and attachment on unpatterned and patterned gels by seeding cardiomyocytes isolated from neonatal rats for the cell alignment and attachment (reprinted with permission from Annabi et al.; copyright (2013), John Wiley & Sons[30]).

2.4. Vessel-on-a-chip

Blood vessels are one of the most important parts of the circulatory system for mammals in particular, which have a closed blood vascular system. In general, blood vessels are of three different types: arteries, which conduct the blood from the heart to the various tissues and organs; veins, which carry blood from tissues and organs to the heart; and finally capillaries, in which the actual exchange of water, chemicals, oxygen, and carbon dioxide takes place between the blood and the tissue fluid. The structure of blood vessels contains three layers, and these are mainly called 'tunica'.[31] The name of the outermost layer is tunica adventitia or tunica external; it is the thickest layer in veins and contains some elastic fibers, mostly collagen, with infiltrated nerve fibers. The tunica media is the middle layer and the thickest layer in arteries that is formed of mainly circularly arranged elastic smooth muscle cells and elastic and collagen fibers. The innermost layer is the thinnest part and named tunica intima, composed of a single layer of simple flattened endothelial cells that are surrounded by subendothelial connective tissue with collagen fiber and smooth muscle cells. Endothelial and smooth muscle cells are important structure parameters of the vessel wall, which also has a crucial role in the pathogenesis of many diseases. A schematic diagram describing a typical artery is shown in Figure 9.[32]

Vascular grafts are used in order to treat damaged, occluded, and diseased arteries. They can have different diameters ranging from millimeters to centimeters with different material types and forms. The compliance (the fractional increase in diameter) and the vascular patency (the condition of being blocked, obstructed or not) are two important parameters for vascular grafts. Some of these values for various vessels

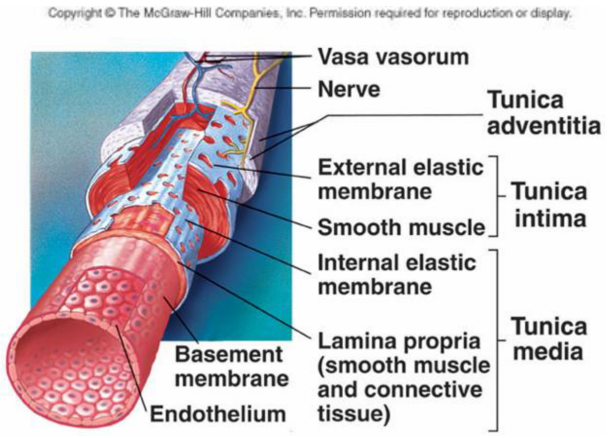


Figure 9. Schematic diagram describing a typical artery with the tunica external, the tunica media, and the tunica intima (reprinted with permission from Shankar; copyright (2016), PathologyOutlines.com [32]).

are demonstrated in the Table. The compliance and the patency performance of vascular grafts made of Dacron and PET and their comparison with some other natural arteries and veins are illustrated here. [33]

Table. Compliance and patency values for various vessels. [33]

	Compliance (% / mmHg × 100)	Patency (%), 1 year	Patency (%), 2 years
Host artery	5.9	...	...
Saphenous vein	4.4	88	84
Umbilical vein	3.7	83	80
Bovine heterograft	2.6	65	59
Dacron	1.9	65	42
PTFE	1.6	60	42

Developing microfluidic devices simulating the biological response of the blood vessels will give us the opportunity for a better comprehensive understanding of the mechanisms behind pathologic changes, responses, and natural functions. Engineered 3D vascular structures can offer many advantages for cell seeding, culturing, and analysis. [34] Recently, several studies have described in vitro human and personalized disease models to develop therapeutic strategies. [35–38] In this regard, a thrombosis-on-chip model using 3D bioprinting technology has been demonstrated. [35] In this model, Pluronic sacrificial micron-sized channels were formed and then coated with a layer of human umbilical vein endothelial cells (HUVECs), and then embedded in GelMA hydrogels. Moreover, in order to mimic human fibrosis and aging, the channels were then coated by fibroblasts whereby they observed that the cells migrated into the clot and deposited collagen type I when the endothelium was damaged. Studying the real situation of the pathology of fibrosis, and especially in thrombosis, in such systems could open up new avenues in medicine.

Additionally, conventional PDMS-based microfluidic channel manufacturing without pretreatment and further modifications might create some challenges when vascular phenomena are explored for cell functioning and behavior under fluid flow for the implementation of drug testing. [36] In this respect, Chung et al. developed a microfluidic platform to study cell migration and behavior under physiological conditions of biophysical, biochemical, and coculture environments. [37] In this study, 3D microenvironments were obtained via soft lithography using PDMS as seen in Figure 10. This model consists of condition (test agents) and control (control

medium) channels in which observation of cell migration, growth factors, and cell polarity demonstrated significant differences. For example, cell migration was faster between the center and condition channels than the control part. However, increasing the collagen gel stiffness for cell adhesion inhibited endothelial cell migration, causing formation of tube-like structures with a diameter of about 20–30 μm even if the cells in softer scaffolds migrated throughout the entire scaffolds. This, in turn, allowed controlling cell behavior by changing the mechanical properties of the scaffold. Researchers also studied the behavior of coculturing endothelial cells with various types of cancer cells that were cultured in the condition channel. This is important since cancer stromal cells can induce capillary formation, angiogenesis, by signaling endothelial cells. In this study, MTLn3 cancer cells attracted human microvascular endothelial cells (HMVECs) that were cultured in the cell channel (Figure 10) for the formation of a capillary structure but the low density of cancer cells could not excite tremendous migration of HMVECs. Furthermore, interactions between vascular smooth muscle cells and endothelial cells, which were cultured in the condition and the cell channels, respectively, were also studied; there was communication between the cells but migration of the endothelial cells was suppressed by smooth muscle cells on both sides of channels although they could migrate only on the control side.

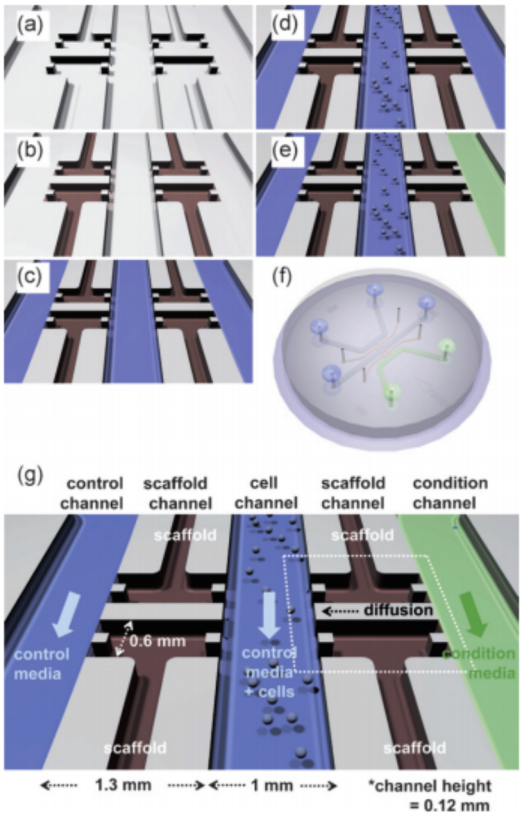


Figure 10. Development of the microscale models: (a) soft lithography and surface treatment; (b) production of cell scaffolds in microchannels (brown represents the gel); (c) filling of the media in the microchannels (blue); (d) the seeding of the cells (spheres) in the central channel; (e) the application of chemical factors (green) in the condition channel; (f) schematic representation of the whole microfluidic device; (g) operational view of 3D microdevice and cell migration behaviors (reprinted with permission from Chung et al.; copyright (2009), The Royal Society of Chemistry [37]).

In another study, Zheng et al. developed a microfluidic flow-stretch chip in order to obtain better mimicking of human biology and explore the cardiovascular system by physical stimulations.[38] To do so, the

effects of fluid shear stress and cyclic stretch created by blood flow and blood pressure on vascular cells and blood vessels' microenvironment, respectively, were investigated.

An additional study was conducted by Kaji et al. in order to monitor the interactions between HeLa cells, a human cervix epithelial cell line, and HUVECs.[39] For this purpose, the group developed a modified type of microfluidic device, which consists of a detachable substrate-based coculture system with glass plate, presensitized (PS) plate, and a PDMS layer, as illustrated in Figure 11. Interactions between the cells were controlled by soluble signaling parameters via coculture of these cell environments. They also developed a system of bubble trapping for the culture medium in order to prevent the negative effect of air bubbles on the cells. The flow direction of the medium was reversed from the HeLa to the HUVEC side and from the HUVEC to the HeLa side. When the HeLa cells were migrated into the areas where HUVECs were already in the space, the HUVECs retreated faster than the HeLa cells migrated. On the other hand, when the second case was applied, in which the flow was from the HUVEC to the HeLa side, interestingly there was a short distance of withdrawal of the HUVECs with a group of the HeLa cells migrating into the HUVECs. There were two groups of these cells interacting and coming into contact during the period of the culture time. Researchers suggest that this different response was probably due to paracrine signaling. As a result, controlling soluble signaling factors secreted from the cell types made the observation of tunable cell migrations and behaviors possible.

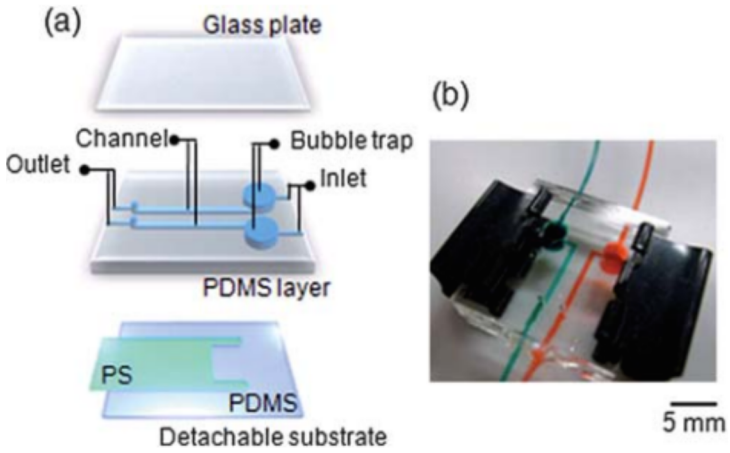


Figure 11. Representation of vessel-on-a-chip device developed by Kaji et al.:[33] (a) schematic of the chip assembly (detachable substrate and PDMS layer with glass plate at the top are bonded together upon plasma treatment); (b) photography image of the assembled device with scale bar of 5 mm (reprinted with permission from Kaji et al.; copyright (2010), The Royal Society of Chemistry[39]).

2.5. Liver-on-a-chip

The liver is located on the right side of the abdomen with two large sections, or lobes, at the right and the left, as illustrated in Figure 12.[40] The lobule and the acinus are important functional units for the structural organization of the human liver.[41] It performs more than 500 functions and many of them are very crucial to sustaining life. Some of these functions can be summarized as removal of toxins (detoxifications), storing of fat-soluble vitamins (A, D, E, and K), and regulation of blood glucose levels while synthesizing clotting factors. It also has an important effect on blood circulation and filtration and the release of bile, proteins, carbohydrate, cholesterol, and so on. All of these important functions make the liver sensitive and vulnerable, especially to adverse effects of certain medications when overdosed and occasionally even at therapeutic ranges. For this

reason, the liver has become a target of drug-induced toxicity and hepatotoxicity. Unfortunately, this also makes the predictions of liver response challenging and hence it is very difficult to mimic the liver in vitro.

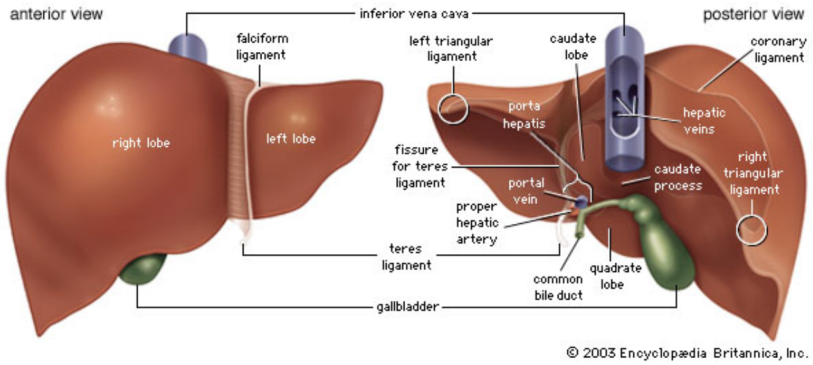


Figure 12. General representation of the human liver and its parts (reprinted with permission from the editors of Encyclopædia Britannica; copyright (2016), Encyclopædia Britannica [40]).

However, building microfluidic devices can still provide useful information for the responses of the human liver when used in drug testing. A couple of researchers have cultured primary hepatocytes in microfluidic devices to accelerate the drug development and screening process. Lee et al. demonstrated the potential use of PDMS-made microfluidic channels for mimicking liver anatomy (Figure 13). [42] For the microfabrication process, epoxy-based negative photoresist (SU-8) for silicone replicate molding with photo-lithography was used to form fluid flow and cell-loading channels. In this study, a cell area was utilized for cell culturing and the medium moved in the flow channel outside of the endothelial-like barrier, partially passing through the endothelial barrier to the cells. Extensive cell–cell contact, continuous nutrient exchange, mimicking of the natural endothelial barrier layer, and culturing of primary hepatocytes for over 7 days without decreasing viability were some important features of the microdevice. On the other hand, the lack of experiments related to waste and toxicity is a downside for the proposed design.

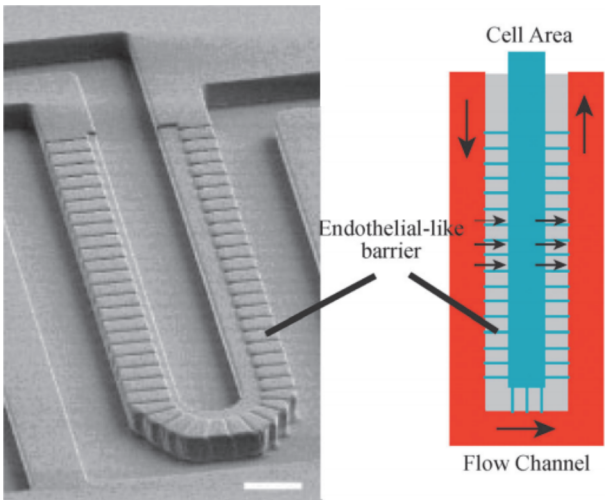


Figure 13. Photograph and schematic representation of in vitro microfluidic liver sinusoid with the endothelial barrier layer (reprinted with permission from Lee et al.; copyright (2007), John Wiley & Sons [42]).

Various studies have also been conducted recently to obtain different types of liver-on-chip microdevices to investigate the potential adverse effects of drugs and treatments. Bhushan and coworkers worked on 3D

microfluidic constructs to mimic functional human liver tissue of the acinus and oxygen gradient that contains four different cell types of hepatocytes, stellate cells, Kupffer cells, and endothelial cells (Figure 14).[43] This chip generates biochemical and metabolic information by the formation of coculturing with synthetic and enzymatic stable functions in at least 4 weeks. Another key point of the model is that the bioengineered chip has fluorescent markers, which can visually indicate changes in cell function when a toxic drug is added to investigate drug-induced liver injury such as fibrotic scarring, cell damage from free radicals, liver failure, and so on. Using such a device, a database, which is the collection of real-time monitoring of changes in cell function, cell death, or damage after drug exposure (Figure 14), can be obtained with clinically relevant hepatotoxic in vivo drug exposure to construct predictive models of human hepatotoxicity.

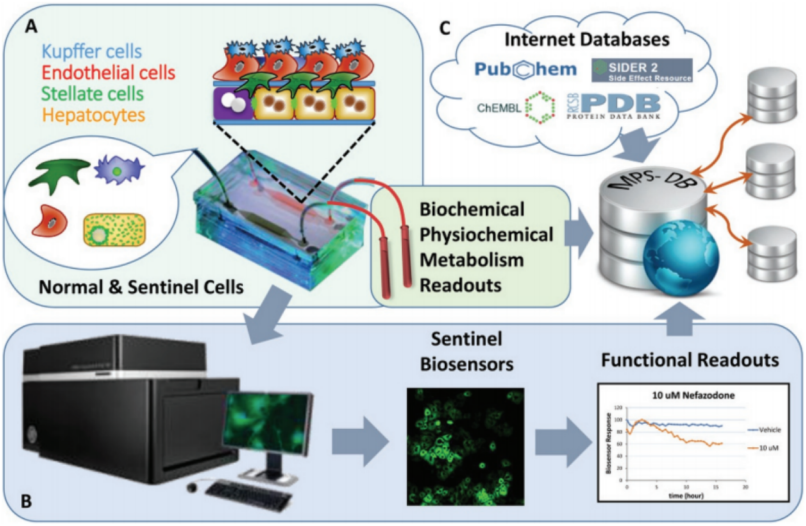


Figure 14. Schematic illustration of developing a liver-on-a-chip to mimic liver acinus: (A) acinus microchip model includes four liver cell types with sentinel cells cultured in the device; (B) investigation of the microchip functions by sentinel biosensors by quantitation readouts; (C) external sources supplied to database with analyzing of graphs and outputs (reprinted with permission from Bhushan et al.; copyright (2013), BioMed Central[43]).

3. 3D bioprinting systems

One of the most important scientific advancements that may provide a high impact on organ-on-a-chip research is the recent progress in 3D bioprinting technologies. Obviously, bioprinting is not the only method to fabricate tissue models for organ-on-chip systems. To date, there have been many strategies employed to fabricate functional tissues, such as 3D scaffolding,[44–47] microengineering based on self-assembly,...[48,49] fiber engineering,[50] and scaffold-free cell sheet engineering,[51] among others.[52,53] Scaffolds, derived from materials like biodegradable polymers, can be refined into desired architectures in 3D, thus allowing the seeded cells to attach, proliferate, migrate, and differentiate.[44,47] Microscale building units such as DNA sequences have the potential to self-assemble into bulk volumes of desired structures that present the properties of the target tissues....[49,54] Fiber engineering based on the cell-laden fibers may also be utilized as the structural units and erected into stratified configurations through weaving, knitting, and spooling....[50,55] Scaffold-free cell sheet engineering depends on accumulating thin sheets of cells layer by layer to fabricate 3D tissue constructs.[51] Despite the fact that all of these strategies have several benefits, none of them have any potential to produce volumetric tissue constructs at high spatial precision.

3D bioprinting is a recently developed biofabrication strategy that is capable of constituting 3D tissue constructs with unprecedented accuracy and remarkable precision in patterning biomaterials and cells in a highly reproducible manner empowered by the programmed fabrication mechanisms....[56−59]

Until recently, a variety of bioprinting strategies have been formulated and fabricated, including those based on stereolithography, inkjet, extrusion, and laser-assisted bioprinting; each comes with their own unique advantages and disadvantages to engineer different types of organ and tissue substitutes. In this section, the most common techniques are outlined in order to emphasize the importance of 3D bioprinting strategies for organ-on-a-chip research.

3.1. Stereolithography bioprinting

In 1986, Charles W Hull described stereolithography bioprinter as an additive manufacturing technique that employs a printhead that can travel on the z-axis and a reservoir filled with cell-laden bioink, which can be selectively solidified layer by layer by photo-polymerization.[60] Stereolithography was first used in medical engineering to biomimic highly accurate and detailed models of the cranium in reconstructive head surgery.[61] In the basic concept of stereolithography bioprinting, 2D patterns are projected onto the bioink layer by layer, resulting in the creation of complex structures without a moveable printhead in the x-y direction and faster fabricating of structures when compared with other nozzle-based bioprinters. This process of photo-polymerization prevents the effect of shear stress on cells and allows bioprinted structures to achieve more than 85% high cell viability. Moreover, this technique does not require highly viscous bioinks and thus extends the choice for biomaterials.[62] A schematic of the photo-polymerization system is shown in Figure 15.[63]

3.2. Inkjet bioprinting

Inkjet bioprinting was invented in 2003 and patented in 2006.[64] An inkjet bioprinter is actually a 2D inkjet printer, where a bioink is used instead of conventional ink and the paper is replaced with an x-y-z controllable platform that allows for the 3D manufacturing of objects (Figure 16a). Bioink is transferred onto the platform through an extruder that is controlled by thermal or piezoelectric actuation. This extrusion allows droplet-wise formation of bioink on the platform and permits the construction of 2D bioprinted layers of desired structure in the z direction. This erection eventually fabricates a 3D object. Simplicity and low cost appear as the most forthcoming advantages of inkjet bioprinting.[60,63] In addition, in inkjet bioprinting, several printheads can work together simultaneously and fabricate high resolution ($\sim$30 μm) structures rapidly.[60,62,64] Also, inkjet bioprinting provides high cell viability ratios of more than 80%–90% in bioprinted structures.[62,65] Gao et al. fabricated an inkjet bioprinter that has the capability to deposit eight materials simultaneously and crosslink the bioprinted structures.[66] This inkjet bioprinter was used to fabricate mechanically strong bone and cartilage constructs using poly(ethylene glycol)dimethacrylate (PEGDMA), GelMA, and encapsulated human mesenchymal stem cells. Moreover, Chang et al. fabricated an inkjet bioprinter that successfully bioprinted bifurcated vascular structures.[67]

3.3. Extrusion-based bioprinting

In 2002, Zein et al. developed the basic principles of extrusion-based 3D bioprinting for tissue engineering for the first time.[68] Poly(ε-caprolactone) (PCL) scaffolds are fabricated through an extrusion-based design with a heating system for extruding the heated and melted material. Pneumatic and mechanical-driven extrusion-based bioprinters appear as the most common versions in the market due to their high performance in tissue

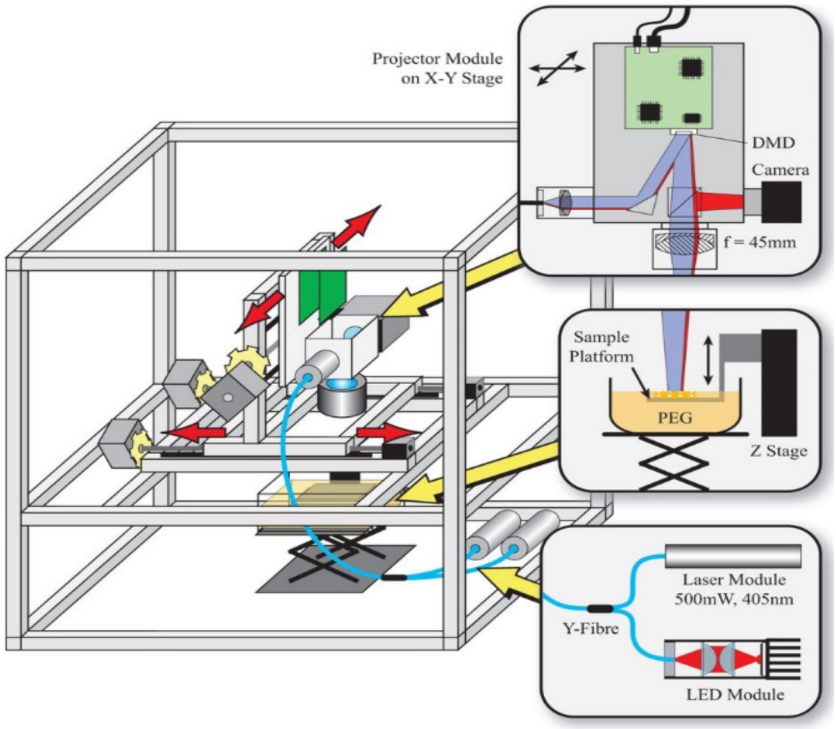


Figure 15. Schematic of the system. An aluminum frame is used to support the custom precision translation stages and projector system. Light from a UV laser and a red LED are combined using a Y-fiber, which is then used to illuminate a Digital Micromirror Device (DMD) projector. A lens is used to project the image of the DMD onto a sample slide, which is immersed in the photopolymer (reprinted with permission from Lee et al.; copyright (2015), Macmillan Publishers Limited[63]).

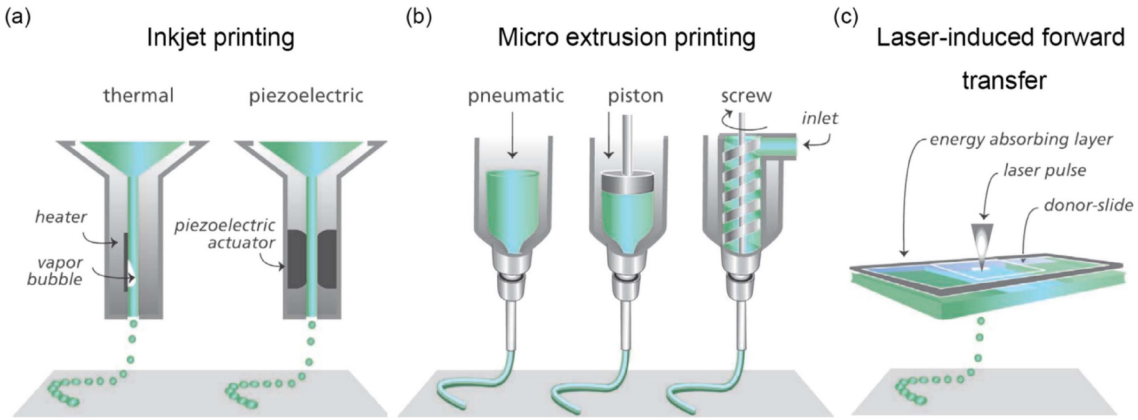


Figure 16. Three most common 3D bioprinting techniques: (a) inkjet bioprinters, (b) microextrusion bioprinters, and (c) laser-assisted bioprinter (reprinted with permission from Malda et al.; copyright (2013), John Wiley & Sons[56]).

engineering (Figure 16b). Pneumatic systems that enable high resolution bioprinting are mainly controlled by valve mechanisms.[69] They provide serious advantages with control over pressure and pulse frequencies. Almost all of the mechanical systems are controlled by a piston or by a screw. Screw-driven systems are mainly preferred for inks with higher viscosities due to higher spatial control. However, it is known that nozzle exits of the screw-driven systems may harm cells because of the high pressure that is applied to them.[69,70] When

extrusion-based bioprinting is compared with other aforementioned platforms, it is obvious that this technique possesses serious advantages, such as the capability of printing highly viscous bioinks (30 MPa s to $>6 \times 10^7$ MPa s) in high cell densities.[62,67,71] Moreover, it should be noted that extrusion-based bioprinting systems have the capacity to extrude bioinks continuously without any interruptions. This is preferred in many applications since the integrity of bioprinted tissue constructs is one of the most important problems to be considered. Therefore, since the invention of extrusion-based bioprinting, this technique has appeared as one of the most widely adopted forms of bioprinting due to its high capability of constructing integrated structures.

3.4. Laser-induced forward transfer bioprinting

Laser-induced forward transfer (LIFT) bioprinting is also known as laser-assisted or laser direct-write bioprinting.[72,73] In 2007, Duocastella et al. published the first paper based on laser-assisted bioprinting and proved the potential of this method for biomedical applications.[74] LIFT bioprinting systems mainly consist of three layers: a donor layer, an energy-absorbing layer, and a layer of bioink (Figure 16c). The donor layer responds to an applied laser beam and this makes it the most crucial part of the system. An energy-absorbing layer such as titanium or gold is attached on top of this donor layer, and at the bottom of the donor layer a thin layer of bioink is suspended. Corresponding locations of the donor layer are vaporized at the moment a selective laser beam is applied to the designed parts of the energy-absorbing layer and thus creates a high-pressure bubble at the interface. This pressure drives bioink in droplet formations onto the collection platforms. Eventually a 3D construct is fabricated by controlling the z stage of the collector. In LIFT bioprinting, the cells are not exposed to high shear stress since there are no contacts between the dispenser and the bioink, resulting in the highest cell viability ratio ($>95\%$) when compared with other aforementioned bioprinting techniques. In addition, this advantage enables LIFT bioprinting to print structures with highly viscous materials (1–300 MPa s).[62,67] By using LIFT, Ali et al. successfully printed mesenchymal stem cells in high resolution with high viability.[75] Recently, Guillemot et al. invented and Guillotin et al. improved LIFT technology and invented a high-throughput laser printing system that successfully achieved a very high cell-level resolution (10 μm) at a very high speed of printing (5 kHz).[76,77] Today, LIFT presents high potential printing capability based on the contactless printing with high speed.

4. Conclusion and future perspectives

The design, development, and then testing of a new drug or treatment is a lengthy process associated with tremendous costs and high failure rates. Traditional approaches like 2D models for monitoring and measuring the effects of the drug on the molecular basis of a disease have many limitations that arise from the more sophisticated nature of real biological systems.[78] As a result of technological advances in the field, the concept of organs-on-chips has been developed, which is expected to mimic specialized organ and immune system responses, reveal correlations between a drug and its toxic effects with lower reagent consumption, and provide better ability to resemble cellular microenvironments.[78–82] In a short period of time, many studies have been carried out to simulate the liver, blood vessels, brain, skin, and so on using microengineered platforms so that at least the minimal functional units of living organs can be artificially modeled and potentially used for biomedical, pharmaceutical, and environmental safety testing applications. Even if there is a need for more multidisciplinary approaches to achieve their full potential before the models become packaged test solutions acceptable to the pharmaceutical industry, there are several important advantages of these models. These can be summarized as:

- Relatively smaller 3D experimental setups with the capability of controlling the positions of cells and tissue–tissue interfaces, transcellular molecules, and their concentration gradient will be advantageous to analyze new drugs-on-chips systems to obtain more accurate results than animal models.[83]
- Organ-on-a-chip systems will potentially replace animal testing, or at least reduce it, thus eliminating the ethical issues often raised by animal rights groups.
- Achievements in the organ-on-a-chip field can reduce the amount of testing determined before and during clinical trials in human patients.[84]
- Combination of gene-replacement technology with the stem cells from an individual patient might lead to personalized medicine or treatment and disease models.[78,85]

On the other hand, the ultimate goal is clearly to develop in vitro model systems of human-on-a-chip that imitate more complex tissue constructs using different types of novel biocompatible materials. However, more sophisticated microsystems are still needed in order to incorporate multiple tissues and vascular channels on a single microdevice since the ultimate goal is to transform fundamental human cells or induced pluripotent stem cells into mature cells while controlling or preventing long-term differentiation to simulate in vivo cell activities precisely.[5,86,87] Almost all microorgan models do not contain enough variety of cells like the mimicked actual organ has, but rather just focus on a single property of cells or cell behaviors, like fusion, ECM–cell interaction, and cell–cell interaction.[88–92] Another issue with the current models is the lack of an intermediate structure or form like the absence of fibroblasts between the endothelial and epithelial tissue of lung-on-a-chip models maintaining the organ-specific cells by proliferation and differentiation capacity.

Organ-on-a-chip systems are still a relatively new area for research and are not yet explored in detail in some biomedical fields such as chronic disease and complicated reactions in the endocrine system or skeletal and nervous systems due to limited working time (i.e. less than a month). For consistent reliability, they should maintain structural integrity after long-term exposure to drugs and biological solutions.

To construct organ-on-a-chip systems, PDMS is widely used currently, but for long-term stability, reliability, better chemical resistance, biocompatibility, reduced absorbance of small hydrophobic molecules on its surface, and solvent effects that seriously affect drug efficacy and toxicity, it should be improved or replaced with new materials.[87,93] Another major drawback of PDMS is the production of membranes that are considerably thicker when compared with real in vivo forms. Based on many experiments, structural integrity is destroyed when the flexible and porous PDMS membrane is produced thinner than 10 μm.[86] Various attempts have been made to find a more suitable alternative material instead of PDMS; however, there is no satisfactory substitute that can potentially replace PDMS-made devices.[80,93]

In order to improve our understanding of specific metabolic and cell–cell interactions with the effect of applying drugs on organ-on-a-chip models, we need mathematical, physical, and simulation models with acceptable accuracy and analysis of complex flows in the cell media. For controllability and long-term usage, automation of organ-on-a-chip systems, monitoring, and data collection points and times need to be standardized and optimized after developing a consensus at least among engineers, pharmacists, and medical doctors. Customized sensors with regeneration capacity and high sensitivity to detect trace changes (<1 ng mL^{-1} or only the target molecule or biomarker in the complex medium) and longer shelf life are also highly demanded.[94]

Alternatively, 3D bioprinting enables us to perform rapid fabrication of organs and tissues in three-dimensional biomimetic structures for applications in tissue engineering and regenerative medicine that may

possibly be associated with organ-on-a-chip systems. It is obvious that in such a case the synergy created by this association will lead to significant advancement for organ-on-a-chip research. However, there are still many challenges on the path towards the development of more viable 3D bioprinting technologies. Unfortunately, none of the tissues and organs are composed of one single cell type. For instance, pacemaker cells lying in the Purkinje fibers initiate the contraction of the heart's chambers and this should be considered when heart tissue is needed for heart-on-a-chip research.[95−97] For liver-on-a chip research, researchers should be aware that hepatocytes are the most crucial elements for liver functions but other nonparenchymal cells like Kupffer cells, hepatic stellate cells, and biliary epithelial cells are also of vital importance.[58,95,98]

In addition, vascularization is another critical component for every living tissue. Perfusable endothelial tubes that have capability to transport nutrients and oxygen among different sections of organs and tissues, and to remove metabolic wastes such as acids and carbon dioxide to maintain the homeostasis of the human body, should be embedded within all fabricated tissue constructs.[99,100] Fabricated tissues and organs have no chance to survive on their own without an interconnected vascular network.

With further development and optimization towards multiplexing organs-on-chips to form human-on-a-chip models, it is highly expected that these systems will find widespread applications in monitoring the effects of drug exposure even at trace amounts and in situ treatments could potentially serve as a replacement for traditional in vivo models.

References

1. Nguyen, N. T.; Shaegh, S. A. M.; Kashaninejad, N.; Phan, D. T. *Adv. Drug Deliver. Rev.* **2013**, *65*, 1403-1419.
2. Weibel, D. B.; Whitesides, G. M. *Curr. Opin. Chem. Biol.* **2006**, *10*, 584-591.
3. Moraes, C.; Mehta, G.; Lesher-Perez, S. C.; Takayama, S. *Ann. Biomed. Eng.* **2012**, *40*, 1211-1227.
4. Moyer, M. W. *Sci. Am.* **2011**, *304*, 19.
5. Ghaemmaghami, A. M.; Hancock, M. J.; Harrington, H.; Kaji, H.; Khademhosseini, A. *Drug Discov. Today* **2012**, *17*, 173-181.
6. Sung, J. H.; Kam, C.; Shuler, M. L. *Lab Chip* **2010**, *10*, 446-455.
7. Esch, M. B.; King, T. L.; Shuler, M. L. *Annu. Rev. Biomed. Eng.* **2011**, *13*, 55-72.
8. Shuler, M. L. *Ann. Biomed. Eng.* **2012**, *40*, 1399-1407.
9. Bhise, N. S.; Ribas, J.; Manoharan, V.; Zhang, Y. S.; Polini, A.; Massa, S.; Dokmeci, M. R.; Khademhosseini, A. *J. Control. Release* **2014**, *190*, 82-93.
10. Leary, J. F.; Key, J.; Vidi, P. A.; Cooper, C. L.; Kole, A.; Reece L. M.; Lelièvre, S. A. *Proc. SPIE* **2013**, *8615*, 86150A.
11. Williamson, A.; Singh, S.; Fernekorn, U.; Schober, A. *Lab Chip* **2013**, *13*, 3471-3480.
12. Sung, J. H.; Esch, M. B.; Prot, J. M.; Long, C. J.; Smith, A.; Hickman, J. J.; Shuler, M. L. *Lab Chip* **2013**, *13*, 1201-1212.
13. Jang, K. J.; Suh, K. Y. *Lab Chip* **2010**, *10*, 36-42.
14. Weinberg, E.; Kaazempur, M. M.; Borenstein, J. *Int. J. Artif. Organs* **2008**, *31*, 508-514.
15. Jang, K. J.; Mehr, A. P.; Hamilton, G. A.; McPartlin, L. A.; Chung, S.; Suh, K. Y.; Ingber, D. E. *Integ. Biol.* **2013**, *5*, 1119-1129.
16. Homan, K. A.; Kolesky, D. B.; Skylar-Scott, M. A.; Herrmann, J.; Obuobi, H.; Moisan, A.; Lewis, J. A. *Sci. Rep.* **2016**, *6*, 34845.
17. Mills, P. R.; Davies, R. J.; Devalia, J. L, *Am. J. Resp. Crit. Care* **1999**, *160*, S38-S43.

18. Hamann, K. J.; Dorscheid, D. R.; Ko, F. D.; Conforti, A. E.; Sperling, A. I.; Rabe, K. F.; White, S. R. *Am. J. Resp. Cell Mol.* **1998**, *19*, 537-542.
19. Tam, A.; Wadsworth, S.; Dorscheid, D.; Man, S. P.; Sin, D. D. *Ther. Adv. Respir. Dis.* **2011**, *5*, 255-273.
20. Huh, D.; Matthews, B. D.; Mammoto, A.; Montoya, Z. M.; Hong, Y. H.; Donald, E. I. *Science* **2010**, *328*, 1662-1668.
21. Nalayanda, D. D.; Puleo, C.; Fulton, W. B.; Sharpe, L. M.; Wang, T. H.; Abdullah, F. *Biomed. Microdevices* **2009**, *11*, 1081-1089.
22. Laizzo, P. A., Ed. *Handbook of Cardiac Anatomy, Physiology, and Devices*; Springer Science & Business Media: New York, NY, USA, 2009.
23. Egert, U.; Meyer, T. In *Practical Methods in Cardiovascular Research*; Dhein, S.; Mohr, F. W.; Delmar, M., Eds. Springer: Berlin, Germany, 2005, pp. 432-453.
24. Grosberg, A.; Alford, P. W.; McCain, M. L.; Parker, K. K. *Lab Chip* **2011**, *11*, 4165-4173.
25. Agarwal, A.; Goss, J. A.; Cho, A.; McCain, M. L.; Parker, K. K. *Lab Chip* **2013**, *13*, 3599-3608.
26. Madden, L. R.; Mortisen, D. J.; Sussman, E. M.; Dupras, S. K.; Fugate, J. A.; Cuy, J. L.; Hauch, K. D.; Laflamme, M. A.; Murry, C. E.; Ratner, B. D. *P. Natl. Acad. Sci. USA* **2010**, *107*, 15211-15216.
27. Shin, S. R.; Jung, S. M.; Zalabany, M.; Kim, K.; Zorlutuna, P.; Kim, S. B.; Nikkhah, M.; Khabiry, M.; Azize, M.; Kong, J. et al. *ACS Nano* **2013**, *7*, 2369-2380.
28. Wheeldon, I.; Ahari, A. F.; Khademhosseini, A. *J. Assoc. Lab. Auto.* **2010**, *15*, 440-448.
29. Naseer, S. M.; Manbachi, A.; Samandari, M.; Walch, P.; Gao, Y.; Zhang, Y. S.; Davoudi, F.; Wang, W.; Abrinia, K.; Cooper, J. M. et al. *Biofabrication* **2017**, *9*, 015020.
30. Annabi, N.; Tsang, K.; Mithieux, S. M.; Nikkhah, M.; Ameri, A.; Khademhosseini, A.; Weiss, A. S. *Adv. Funct. Mater.* **2013**, *23*, 4950-4959.
31. Porth, C. *Essentials of Pathophysiology: Concepts of Altered Health States*; Lippincott Williams & Wilkins: Philadelphia, PA, USA, 2011, pp. 405-407.
32. Shankar, V. *Degenerative Joint Disease*, 2016. Available online at http://www.pathologyoutlines.com/topic/ joints-DJD.html.
33. Mizelle, S. W. MSc, North Carolina State University, Raleigh, NC, USA, 1997.
34. Van der Meer, A. D.; Poot, A. A.; Duits, M. H. G.; Feijen, J.; Vermes, I. *J. Biomed. Biotechnol.* **2009**, *2009*, 823148.
35. Zhang, Y. S.; Davoudi, F.; Walch, P.; Manbachi, A.; Luo, X.; Dell'Erba, V.; Miri, A. K.; Albadawi, H.; Arneri, A.; Li, X. et al. *Lab Chip* **2016**, *16*, 4097-4105.
36. Zheng, Y.; Chen, J.; Craven, M.; Choi, N. W.; Totorica, S.; Diaz-Santana, A.; Kermani, P.; Hempstead, B.; Fischbach-Teschl, C.; López, J. A. et al. *P. Natl. Acad. Sci. USA* **2012**, *109*, 9342-9347.
37. Chung, S.; Sudo, R.; Mack, P. J.; Wan, C. R.; Vickerman, V.; Kamm, R. D. *Lab Chip* **2009**, *9*, 269-275.
38. Zheng, W.; Jiang, B.; Wang, D.; Zhang, W.; Wang, Z.; Jiang, X. *Lab Chip* **2012**, *12*, 3441-3450.
39. Kaji, H.; Yokoi, T.; Kawashima, T.; Nishizawa, M. *Lab Chip* **2010**, *10*, 2374-2379.
40. Editors of Encyclopædia Britannica. *Liver* In *Encyclopædia Britannica*; Encyclopædia Britannica: London, UK, 2016**.**
41. Arias, I.; Wolkoff, A.; Boyer, J.; Shafritz, D.; Fausto, N.; Alter, H.; Cohen, D., Eds. *The Liver: Biology and Pathobiology*; John Wiley & Sons: Hoboken, NJ, USA, 2011.
42. Lee, P. J.; Hung, P. J.; Lee, L. P. *Biotechnol. Bioeng.* **2007**, *97*, 1340-1346.
43. Bhushan, A.; Senutovitch, N.; Bale, S. S.; McCarty, W. J.; Hegde, M.; Jindal, R.; Golberg, I.; Usta, O. B.; Yarmush, M. L.; Vernetti, L. et al. *Stem Cell Res. Ther.* **2013**, *4*, S16.
44. Zhang, Y. S.; Xia, Y. *Nanomedicine* **2015**, *10*, 689-692.
45. Zhang, Y. S.; Choi, S. W.; Xia, Y. *Soft Matter* **2013**, *9*, 9747-9754.

46. Wade, R. J.; Burdick, J. A. *Nano Today* **2014**, *9*, 722-742.
47. Owen, S. C.; Shoichet, M. S. *J. Biomed. Mater. Res. A* **2010**, *94*, 1321-1331.
48. Khademhosseini, A.; Langer, R. *Biomaterials* **2007**, *28*, 5087-5092.
49. Du, Y.; Lo, E.; Ali, S.; Khademhosseini, A. *P. Natl. Acad. Sci. USA* **2008**, *105*, 9522-9527.
50. Onoe, H.; Okitsu, T.; Itou, A.; Kato-Negishi, M.; Gojo, R.; Kiriya, D.; Sato, K.; Miura, S.; Iwanaga, S.; Kuribayashi-Shigetomi, K. et al. *Nat. Mater.* **2013**, *12*, 584-590
51. Yamato, M.; Okano, T. *Mater. Today* **2004**, *7*, 42-47.
52. Place, E. S.; Evans, N. D.; Stevens, M. M. *Nat. Mater.* **2009**, *8*, 457-470.
53. Atala, A.; Kasper, F. K.; Mikos, A. G. *Sci. Transl. Med.* **2012**, *4*, 160rv12.
54. Matsunaga, Y. T.; Morimoto, Y.; Takeuchi, S. *Adv. Mater.* **2011**, *23*, H90-H94.
55. Kang, E.; Jeong, G. S.; Choi, Y. Y.; Lee, K. H.; Khademhosseini, A.; Lee, S.H. *Nat. Mater.* **2011**, *10*, 877-883.
56. Malda, J.; Visser, J.; Melchels, F. P.; Jüngst, T.; Hennink, W. E.; Dhert, W. J.; Groll, J.; Hutmacher, D. W. *Adv. Mater.* **2013**, *25*, 5011-5028.
57. Li, Y. C.; Zhang, Y. S.; Akpek, A.; Shin, S. R.; Khademhosseini, A. *Biofabrication* **2016**, *9*, 012001.
58. Zhang, Y. S.; Yue, K.; Aleman, J.; Mollazadeh-Moghaddam, K.; Bakht, S. M.; Yang, J.; Jia, W.; Dell'Erba, V.; Assawes, P.; Shin, S. R. et al. *Ann. Biomed. Eng.* **2017**, *45*, 148-163.
59. Murphy, S. V.; Atala, A. *Nat. Biotechnol.* **2014**, *32*, 773-785.
60. Hull, C. W. *U.S. Patent No. 4,575,330*; US Patent Office: Washington, DC, USA, 1986.
61. Klimek, L.; Klein, H. M.; Schneider, W.; Mösges, R.; Schmelzer, B.; Voy, E. D. *Acta Otorhinolaryngo. Belg.* **1992**, *47*, 329-334.
62. Mandrycky, C.; Wang, Z.; Kim, K.; Kim, D. H. *Biotechnol. Adv.* **2016**, *34*, 422-434.
63. Lee, M. P.; Cooper, G. J.; Hinkley, T.; Gibson, G. M.; Padgett, M. J.; Cronin, L. *Sci. Rep.* **2015**, *5*, 9875.
64. Boland, T.; Wilson, W. C.; Xu, T. *U.S. Patent No 7051654 B2*; US Patent Office: Washington, DC, USA, 2003.
65. Wilson, W. C.; Boland, T. *Anat. Rec. Part A* **2003**, *272*, 491-496.
66. Gao, G.; Schilling, A. F.; Hubbell, K.; Yonezawa, T.; Truong, D.; Hong, Y.; Dai, G.; Cui, X. *Biotechnol. Lett.* **2015**, *37*, 2349-2355.
67. Chang, C. C.; Boland, E. D.; Williams, S. K.; Hoying, J. B. *J. Biomed. Mater. Res. B* **2011**, *98*, 160-170.
68. Zein, I.; Hutmacher, D. W.; Tan, K. C.; Teoh, S. H. *Biomaterials* **2002**, *23*, 1169-1185.
69. Ozbolat, I. T.; Hospodiuk, M. *Biomaterials* **2016**, *76*, 321-343.
70. Fielding, G. A.; Bandyopadhyay, A.; Bose, S. *Dent. Mater.* **2012**, *28*, 113-122.
71. Murphy, S. V.; Skardal, A.; Atala, A. *J. Biomed. Mater. Res. A* **2013**, *101*, 272-284.
72. Bohandy, J.; Kim, B. F.; Adrian, F. J. *J. Appl. Phys.* **1986**, *60*, 1538-1539.
73. Kattamis, N. T.; Purnick, P. E.; Weiss, R.; Arnold, C. B. *Appl. Phys. Lett.* **2007**, *91*, 171120.
74. Duocastella, M.; Colina, M.; Fernández-Pradas, J. M.; Serra, P.; Morenza, J. L. *Applied Surf. Sci.* **2007**, *253*, 7855-7859.
75. Ali, M.; Pages, E.; Ducom, A.; Fontaine, A.; Guillemot, F. *Biofabrication* **2014**, *6*, 045001.
76. Guillemot, F.; Souquet, A.; Catros, S.; Guillotin, B.; Lopez, J.; Faucon, M.; Pippenger, B.; Bareille, R.; Rémy, M.; Bellance, S. et al. *Acta Biomater.* **2010**, *6*, 2494-2500.
77. Guillotin, B.; Souquet, A.; Catros, S.; Duocastella, M.; Pippenger, B.; Bellance, S.; Bareille, R.; Rémy, M.; Bordenave, L.; Amédée, J. et al. *Biomaterials* **2010**, *31*, 7250-7256.
78. Bhatia, S. N.; Ingber, D. E. *Nat. Biotechnol.* **2014**, *32*, 760-772.
79. Huh, D.; Torisawa, Y.; Hamilton, G. A.; Kim, H. J.; Ingber, D. E. *Lab Chip* **2012**, *12*, 2156-2164.

80. Esch, M. B.; Sung, J. H.; Shuler, M. L. *J. Biotechnol.* **2010**, *148*, 64-69.

81. Shin, S. R.; Kilic, T.; Zhang, Y. S.; Avci, H.; Hu, N.; Kim, D., Branco, C.; Aleman, J.; Massa, S.; Silvestri, A. et al. *Adv. Sci.* **2017**, *4*, 1-14.

82. Zhang, Y. S.; Aleman, J.; Shin, S. R.; Kilic, T.; Kim, D.; Shaegh, S. A. M.; Massa, S., Riahi, R.; Chae, S.; Hu, N. et al. *P. Natl. Acad. Sci. USA* **2017**, *114*, E2293-E2302.

83. Kim, S.; Takayama, S. *Kidney Res. Clin. Pract.* **2015**, *34*, 165-169.

84. Esch, E. W.; Bahinski, A.; Huh, D. *Nat. Rev. Drug Discov.* **2015**, *14*, 248-260.

85. Wang, G.; McCain, M. L.; Yang, L.; He, A.; Pasqualini, F. S.; Agarwal, A.; Yuan, H.; Jiang, D.; Zhang, D.; Zangi, L. et al. *Nat. Med.* **2014**, *20*, 616-623.

86. Huh, D.; Kim, H. J.; Fraser, J. P.; Shea, D. E.; Khan, M.; Bahinski, A.; Hamilton, G. A.; Ingber, D. E. *Nat. Protoc.* **2013**, *8*, 2135-2157.

87. Huh, D.; Hamilton, G. A.; Ingber, D. E. *Trends Cell Biol.* **2011**, *21*, 745-754.

88. Yang, X.; Mironov, V.; Wang, Q. *J. Theor. Biol.* **2012**, *303*, 110-118.

89. Yang, X., Sun, Y., Wang, Q. *J. Biomech. Eng.* **2013**, *135*, 71005.

90. Thomas, G. L.; Mironov, V.; Nagy-Mehez, A.; Mombach, J. C. M. *Physica A* **2014**, *395*, 247-254.

91. Ki, C. S.; Lin, T. Y.; Korc, M.; Lin, C. C. *Biomaterials* **2014**, *35*, 9668-9677.

92. Abdulla, T.; Imms, R. A.; Schleich, J. M.; Summers, R. In *Proceedings of the 33rd Annual International Conference of the IEEE EMBS*, Boston, MA, USA, 30 August–3 September 2011, pp. 449-452.

93. Sackmann, E. K.; Fulton, A. L.; Beebe, D. J. *Nature* **2014**, *507*, 181-189.

94. Shin, S.; Zhang, Y. S.; Kim, D.; Manbohi, A.; Avci, H.; Silvestri, A.; Aleman, J.; Hu, N.; Kilic, T.; Keung, W. et al. *Anal. Chem.* **2016**, *88*, 10019-10027.

95. Saladin, K. S.; Miller L. *Anatomy & Physiology: The Unity of Form and Function*; McGraw-Hill: New York, NY, USA, 1998.

96. Zhang, Y. S.; Aleman, J.; Arneri, A.; Bersini, S.; Piraino, F.; Shin, S. R.; Dokmeci, M. R.; Khademhosseini, A. *Biomed. Mater.* **2015**, *10*, 034006.

97. Tomanek, R. J.;. Runyan, R. B., Eds. *Formation of the Heart and Its Regulation*; Birkhäuser: Boston, MA, USA, 2012.

98. Langer, R.; Vacanti, J. P.; Vacanti, C. A.; Atala, A.; Freed, L. E.; Vunjak-Novakovic, G. *Tissue Eng.* **1995**, *1*, 151-161.

99. Bae, H.; Puranik, A. S.; Gauvin, R.; Edalat, F.; Carrillo-Conde, B.; Peppas, N. A.; Khademhosseini, A. *Sci. Transl. Med.* **2012**, *4*, 160ps23.

100. Lovett, M.; Lee, K.; Edwards, A.; Kaplan, D. L. *Tissue Eng. Pt. B-Rev.* **2007**, *15*, 353-370.